Chromatin modifiers in DNA repair and human disease

Helfricht, A.

4

INVESTIGATING DNA DAMAGE-INDUCED RSF1 SUMOYLATION

Angela Helfricht[1], Karolin Eifler-Olivi[2],
Haico van Attikum[1] and Alfred C. Vertegaal[2]

[1] Department of Human Genetics, Leiden University Medical Center
[2] Department of Molecular Cell Biology, Leiden University Medical Center

ABSTRACT

The small ubiquitin-like modifier (SUMO) has been described to regulate the activity, stability and /or interactions of numerous proteins within the DNA damage response (DDR) including the Remodeling and Spacing Factor 1 (RSF1). RSF1 is extensively SUMOylated, as evidenced by the identification of 21 SUMO-acceptor lysines, and has been implicated in facilitating repair of DNA double-strand breaks (DSBs) by promoting the incorporation of centromere proteins CENP-S and CENP-X into the damaged chromatin. Here, we show the DNA damage-regulated SUMOylation of endogenous RSF1 in time after exposure of human cells to ionizing radiation (IR). A SUMO-deficient RSF1 mutant, containing 21 lysine to arginine (21KR) point mutations, appeared to be incapable of recruiting the key DSB repair factor XRCC4 of the non-homologous enjoining pathway (NHEJ) to chromatin, although this RSF1 mutant was still recruited to DSB-containing laser tracks. Consequently, this suggests that the DNA damage-dependent SUMOylation of RSF1 is dispensable for the accumulation of RSF1, but it is likely required for XRCC4 accrual to DSBs.

INTRODUCTION

The Remodeling and Spacing Factor 1 (RSF1) is a histone chaperone that has been described to form the RSF complex together with the chromatin remodelling ATPase SWI/SNF-related matrix-associated actin-dependent regulator of chromatin subfamily A member 5 (SMARCA5/SNF2h) of the ISWI family. SMARCA5 has been shown to physically associate with the E3 ubiquitin-protein ligase RNF168 upon DNA damage-induction and to promote the formation of RNF168-dependent ubiquitin conjugates, which facilitate the recruitment of downstream DNA double-strand break (DSB) response factors such as the Breast cancer type 1 susceptibility protein (BRCA1). Moreover, SMARCA5 is required for the proper execution of the two major DSB repair pathways i.e. nonhomologous end-joining (NHEJ) and homologous recombination (HR) (Lan et al., 2010; Smeenk et al., 2013).

More recently, we and others have shown a role for RSF1 in the cellular response to DNA damage. RSF1 is recruited to DSBs in an Ataxia telangiectasia mutated (ATM)-dependent fashion, but unexpectedly, its recruitment did not require its binding partner SMARCA5 (Helfricht et al., 2013; Min et al., 2014; Pessina and Lowndes, 2014). At DSBs, RSF1 deposits the centromere proteins CENP-S and CENP-X and thereby promotes the recruitment of the important DSB-repair factor X-ray repair cross-complementing protein 4 (XRCC4) of the NHEJ pathway (Helfricht et al., 2013). Interestingly, RSF1 also promotes the mono-ubiquitylation of the Fanconi Anemia proteins FANCD2 and FANCI upon DNA damage induction (Pessina and Lowndes, 2014). Thus, RSF1 contributes to a permissive chromatin state to allow efficient DNA repair by at least two mechanisms.

Proteins in the DNA damage response (DDR) are extensively regulated by post-translational modifications, including ubiquitin and small ubiquitin-like modifier (SUMO) (Jackson and Durocher, 2013). Similar to ubiquitin, SUMO is present in an inactive precursor state in cells and needs to be processed by specific proteases to become the mature protein. Conjugation of SUMO to a target protein is an ATP-dependent reaction and is catalysed by an enzymatic cascade. In humans the first step is mediated by the heterodimeric SUMO-activating enzyme (SAE1/SAE2), often indicated as the SUMO E1 enzyme. Once activated, SUMO is transferred to the SUMO-conjugating or E2 enzyme Ubiquitin carrier protein 9 (UBC9), which selects and binds directly to a SUMOylation consensus site in any of the target proteins (Flotho and Melchior, 2013). The common SUMOylation consensus motif starts with a large hydrophobic residue followed by the SUMO acceptor lysine and contains a glutamic acid two positions downstream of the SUMOylated lysine (Hendriks et al., 2014; Matic et al., 2010). Other SUMOylation motifs include the inverted consensus motif [(ED)xKx(≠ED)] (E: glutamic acid; D: aspartic acid, K: lysine) and a hydrophobic cluster motif (Matic et al., 2010).

The most efficient way for assuring substrate specificity is achieved by an E3 enzyme or SUMO ligase, which can transfer SUMO from the E2 onto a specific substrate (Flotho and Melchior, 2013). The SUMO E3 ligases PIAS1 and PIAS4 have been shown to be recruited to DSBs and to promote the accrual of SUMO at the site of DNA damage thereby facilitating the recruitment of 53BP1 and BRCA1 (Galanty et al., 2009).

In human cells, 3 different modifiers are distinguished, SUMO-1, -2 and -3. SUMO-2 and SUMO-3 are virtually identical and are also the most abundant SUMO family members (Saitoh and Hinchey, 2000). Furthermore, SUMO-2 and SUMO-3 contain an internal SUMOylation site, enabling SUMO-chain formation. In contrast, SUMO-1 is missing this internal SUMOylation motif and therefore can function as a chain-terminator when being included in SUMO polymers.

Since SUMO is attached covalently to lysine residues in substrates, it potentially competes with other lysine-directed posttranslational modifications like poly(ADP-ribosyl)ation (PARylation), methylation, acetylation or ubiquitylation (Hendriks et al., 2014). Moreover, SUMOylation has distinct roles; it can promote protein-protein interactions, or interfere with protein-protein interactions due to steric hindrance (Flotho and Melchior, 2013; Jentsch and Psakhye, 2013). In addition proteins containing one or more SUMO-interacting motifs (SIMs) formed by a stretch of hydrophobic amino acids or a specific ZZ zinc finger, are able to bind to SUMO (Danielsen et al., 2012; Song et al., 2004).
SUMOylation is involved in numerous cellular processes including the DDR, but mechanistic understanding of its mode of action is hampered by the lack of detailed knowledge of its substrates. PIAS4-mediated SUMOylation plays a crucial role during the ubiquitylation-dependent signalling of DSBs. Notably, the SUMOylation of HERC2 facilitates the interaction of HERC2 with RNF8, and the assembly of UBC13 with RNF8 thereby promoting DNA damage-induced formation of Lys 63-linked ubiquitin chains, while the SUMOylation of RNF168 actually promotes its own recruitment to DSBs (Bekker-Jensen et al., 2010; Danielsen et al., 2012). Moreover, the DNA damage-induced SUMOylation of the early DSB response factor MDC1 might provide potential binding sites for RAP80 and thereby stimulate the subsequent BRCA1 assembly (Hu et al., 2012; Luo et al., 2012; Strauss and Goldberg, 2011; Strauss et al., 2011). On the contrary, MDC1-SUMOylation on lysine 1840 by PIAS4 is required for its removal from DNA lesions through the SUMO-dependent recruitment of the SUMO-targeted ubiquitin ligase (STUbL) RNF4, which targets MDC1 for degradation (Luo et al., 2012). In addition, the ubiquitin E3 ligase activity of BRCA1 is increased upon SUMOylation (Hu et al., 2012; Morris et al., 2009).
Novel SUMOylation acceptor lysines identified recently (Hendriks et al., 2014; Matic et al., 2010) disclosed RSF1 as a SUMOylation target (Hendriks et al., 2014; Hendriks et al., 2015; Matic et al., 2010). In this study we used straight-forward immunoprecipitation methods to show the SUMOylation of RSF1 upon exposure to ionizing radiation (IR) and investigated the functional relevance of RSF1 SUMOylation, by generation of a SUMO-deficient mutant (K21R). This RSF1 K21R mutant was less capable to target XRCC4 to a LacO-array enriched with RSF1 21KR in a DNA damage-independent assay compared to wild-type RSF1. We thus speculate that RSF1 SUMOylation may be critical to promote XRCC4 loading at DSBs during NHEJ.

RESULTS

RSF1 is SUMOylated upon DNA-damage induction

We recently showed that RSF1 regulates NHEJ by promoting the recruitment of the core DNA repair factor XRCC4 through the deposition of the centromeric proteins CENP-S and CENP-X (Helfricht et al., 2013). At the same time, proteomic studies identified RSF1 as a potential SUMO-2 target protein (Hendriks et al., 2014; Matic et al., 2010) raising the question whether RSF1's role in DNA repair is regulated by SUMOylation. To this end, we monitored ionizing radiation (IR)-induced SUMOylation of RSF1 in U2OS cells at different time points after DNA damage induction. In these experiments we used U2OS cells stably expressing FLAG-SUMO-2 and anti-FLAG immunoprecipitation (IP) to enrich for SUMO-2 conjugates as well as parental U2OS cells (Schimmel et al., 2014), to investigate the SUMOylation levels of endogenous RSF1 upon exposure of cells to IR. SUMOylated forms of RSF1 were detected by

western blot running slightly higher than endogenous RSF1. A clear increase in SUMOylated RSF1 was detected already 0.5 h after exposure of cells to IR (Fig. 1A). The SUMOylation increase was even more pronounced after 2 hours, while the IP of SUMO-2 conjugates was equally efficient (Fig. 1A). In this particular experiment, the levels of endogenous RSF1 in the input samples decreased over time upon irradiation, but additional experiments revealed that the detected decrease in RSF1 expression was not observed reproducibly (Fig. S1A) and ruled out that RSF1 was degraded by the proteasome (data not shown).
Furthermore, we tried to detect SUMOylation of overexpressed GFP-RSF1, since GFP-RSF1 wt could serve as control in experiments employing an RSF1 SUMO mutant. We therefore transfected parental HeLa cells or HeLa cells stably expressing His6-SUMO-2 with either a control plasmid or a plasmid encoding GFP-RSF1 and performed a His-pulldown (PD) to enrich for SUMO conjugates. Consistent with our previous results, we could detect a strong SUMOylation signal for GFP-RSF1, but not in control PD samples (Fig. 1B). SUMOylated full-length GFP-RSF1 appeared in a typical SUMO ladder-type of signal above the marked GFP-RSF1 band (*). However additional lower molecular weight SUMOylation bands were detected on the immunoblot before and after His-PD, which suggest that ectopically expressed GFP-RSF1 got partially degraded in the absence of DNA damage (Fig. 1B).

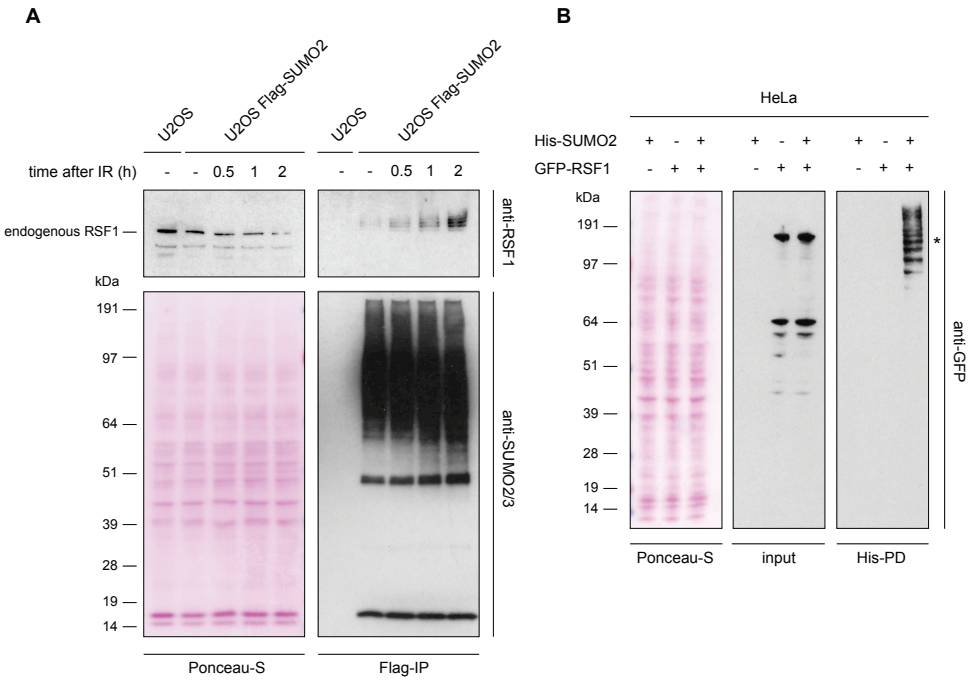

Figure 1. RSF1 is SUMOylated upon DSB induction. (A) Immunoblot analysis of total lysates and Flag-IP samples from U2OS cells stably expressing Flag-SUMO-2 or parental control cells, which were mock treated or exposed to 4 Gy of IR and lysed after the indicated time points. The SUMOyation of endogenous RSF1 is shown, while Ponceau-S stain serves as a loading control and SUMO-2/3-levels show IP-efficiency. (B) HeLa cells stably expressing His-tagged SUMO-2 or parental control cells, were transfected with a control or the indicated plasmid 24 h prior to cell lysis. Total lysates were subjected to His-PD procedure enriching SUMO-2 conjugates. Precipitates were visualized using anti-GFP antibody during immunoblot analysis. Ponceau-S staining is included as loading control. * marks full-length GFP-RSF1.

SUMOylation of the RSF1 21KR mutant is abrogated

RSF1 is a protein with two functional domains, a DNA binding homeobox and Different Transcription factors (DDT) domain at the N-terminus facilitating DNA binding, and a PhD-type Zinc-finger towards the C-terminus of the protein (Fig. 2A). A significant number of lysines in the RSF1 amino acid (aa) sequence have been identified as SUMO acceptor lysines, making it one of the most extensively SUMOylated proteins described so far (Hendriks et al., 2014; Matic et al., 2010). Through site-directed mutagenesis we introduced point mutations to replace 21 lysines (K) for arginines (R). Arginine has been selected as a replacement for lysine, since both amino acids contain positively charged side chains and only one mutation per codon was necessary to mediate the amino acid change. The position of all 21 aa conversions of the RSF1 21KR mutant are distributed over a region between the more N-terminally located K243 and the K768 of the 1441 aa counting RSF1 sequence and are not positioned within one of the described functional domains (Fig. 2A, Table S1). Plasmids encoding GFP fusions of RSF1 wt or the 21KR mutant, or encoding GFP only as a negative control, were transiently expressed in U2OS cells stably expressing His-SUMO-2. Cell lysates were subjected to the His-PD procedure to enrich for SUMO conjugates. While the PD was equally efficient, only GFP-RSF1 wt was SUMOylated, but the GFP-RSF1 21KR mutant was not (Fig. 2B and Fig. S1B). This indicates that point mutations of the RSF1 21KR mutant led to its loss of SUMOylation. Interestingly, previous mass spectrometry studies had identified six SUMO acceptor sites in RSF1 and revealed K294 as the most abundant one (Matic et al., 2010). We therefore created a K294R mutant and a 6KR RSF1 mutant at first, however these mutants were still SUMOylated similar to wild-type RSF1 (data not shown).

The RSF1 21KR mutant is recruited to laser tracks

RSF1 was shown to be recruited to DSBs in a manner dependent on ATM (Helfricht et al., 2013; Min et al., 2014; Pessina and Lowndes, 2014). To investigate whether SUMOylation of RSF1 plays a role in its recruitment to DSBs, we inflicted DNA damage by laser micro-irradiation in U2OS cells transiently expressing either GFP-RSF1 wt or the 21KR mutant. Interestingly both, RSF1 wt and 21KR were rapidly recruited to DSB-containing laser tracks with similar kinetics (Fig. 2C,D). This indicates that the SUMOylation of RSF1 is not important for its recruitment to DSBs and that the laser dependent recruitment of RSF1 was compromised by the replacement of 21 lysines to arginines.

XRCC4 accumulation is hampered in the RSF1 21KR mutant

Since we have shown that RSF1 promotes NHEJ repair by loading of XRCC4 onto DSB-containing chromatin (Helfricht et al., 2013), it is an obvious question whether the RSF1 21KR mutant is still capable to promote XRCC4 loading onto chromatin. We therefore generated mCherry-LacR-RSF1 wt and mCherry-LacR-21KR fusions, which upon expression in U2OS cells containing a LacO array (U2OS 2-6-3) were targeted through the binding of LacR to the array (Luijsterburg et al., 2012; Soutoglou and Misteli, 2008). To suppress endogenous RSF1 expression, U2OS 2-6-3 cells were treated with a siRNA against RSF1 prior to co-expression of siRNA-resistant mCherry-LacR-RSF1 and GFP-XRCC4. By means of mCherry fused to LacR, we could visualize the targeting of mCherry-LacR-NLS (neg. control) as well as mCherry-LacR -RSF1 wt and mCherry-LacR- 21KR to the array and subsequently monitored GFP-XRCC4 accumulation (Fig. 3A). XRCC4 did not accumulate at the LacO array in the absence of RSF1, as has been shown in chapter 3 Fig. 6. But XRCC4 clearly assembled at RSF1 wt covered arrays, while in comparison the amount of XRCC4 detected at targeted RSF1 21KR was

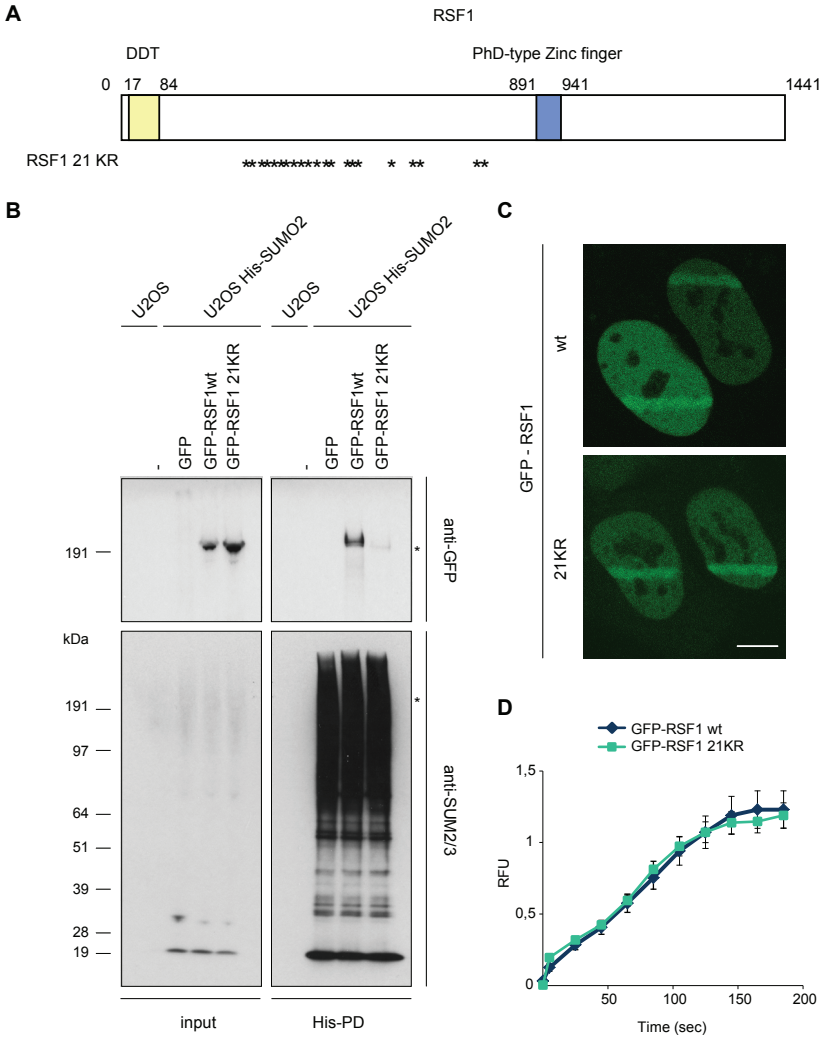

Figure 2. The RSF1 21KR mutant does not get SUMOylated. (A) Overview of full-length human RSF1 amino acid (aa) sequence. 21 K to R mutation positions are indicated by asterisks. (B) U2OS cells stably expressing His-SUMO-2 or parental control cells were either mock treated or transfected with the indicated plasmids. 24 h after transfection, lysates were prepared and analysed by immunoblotting using anti GFP antibody and anti SUMO-2/3 antibody. SUMO-2/3 levels show equal PD efficiency and equal loading. GFP signals indicate GFP-tagged RSF1 wt or 21KR. The asterisks shows the location of full-length GFP-RSF1 on the blot. (C) Live cell microscopy experiment: U2OS cells were transiently transfected with GFP-RSF1 wt or 21KR. Cells were subjected to local laser micro-irradiation and monitored in time. Representative images are shown for the 180 sec time point. The scale bar indicates 10 µm. (D) Quantification of GFP-RSF1 recruitment to DNA-damage containing laser tracks from cells in (C) presented in Relative Fluorescent Units (RFU) over time.

decreased by approximately 75% (Fig. 3B). This suggests a role for SUMOylation of RSF1 in the recruitment of XRCC4 to chromatin.

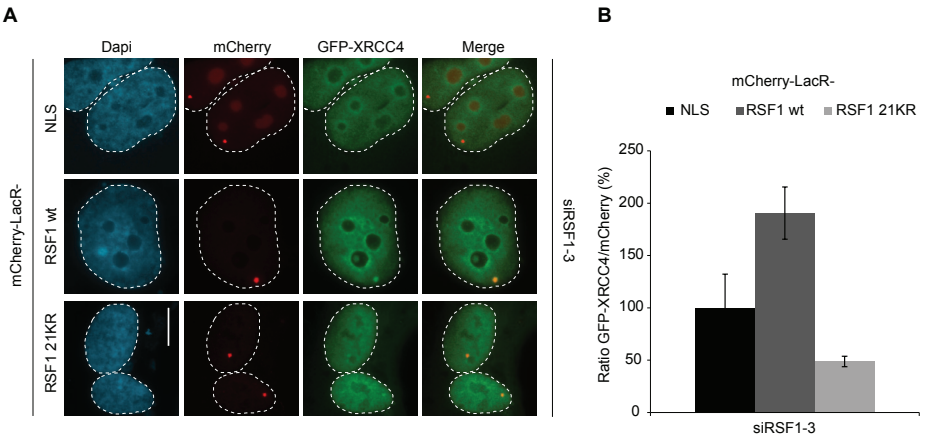

Figure 3. XRCC4 targeting is strongly decreased upon expression of RSF1 21KR mutant. (A) U2OS 2-6-3 cells containing 256 copies of a LacO repeat were treated with siRSF1-3. 48 h later, cells were co-transfected with the indicated mCherry-LacR-fusion plasmids and GFP-XRCC4. After additional 24 h, cells were fixed and stained with Dapi. Representative images are shown for mCherry-fusion constructs targeted to the LacO array and subsequent GFP-XRCC4 recruitment. The scale bar indicates 10 µm. (B) Quantification of the signal intensity of DNA-damage independent recruitment of GFP-XRCC4 to mCherry-LacR-fusions located at the LacO array from cells in (A). The ratio of GFP-XRCC4 over the mCherry-LacR-fusions from two independent experiments with more than 60 cells analysed per condition is presented. Error bars indicate the standard error of the mean (s.e.m).

DISCUSSION

SUMOylation is a post-translational modification (PTM) that can change the stability of a protein, its localization or interactions when it is attached to a substrate. Since RSF1 was identified as a SUMO target protein (Hendriks et al., 2015; Matic et al., 2010) and implicated in the DNA damage response (Helfricht et al., 2013; Min et al., 2014; Pessina and Lowndes, 2014), we initiated an investigation to determine the role of RSF1 SUMOylation during DSB repair. Here we demonstrate for the first time the DNA damage-dependent SUMOylation of endogenous RSF1 (Fig. 1A). In order to assess the impact of SUMOylation on RSF1 function, we generated the RSF1 21KR SUMO mutant, which comprised 21 lysine to arginine point mutations and was deficient in RSF1 SUMOylation. While this mutant was still recruited to laser-induced DNA damage (Fig. 2C,D) with similar kinetics as RSF1 wt, its ability to load XRCC4 was highly decreased (Fig. 3A,B).

The RSF1 21KR mutant

Recently, several SUMO acceptor lysines had been found in RSF1 (Hendriks et al., 2014; Hendriks et al., 2015; Matic et al., 2010), hence we generated several RSF1 SUMO mutants. In contrast to the 21KR mutant, the RSF1 K294K and 6KR mutants did not show reduced SUMOylation levels (data not shown) and for that reason were excluded from further experimental testing. Importantly, when introducing lysine to arginine mutations, not only SUMO acceptor sites might be disrupted, but also acceptor lysines for other PTMs might be lost, which could influence one or more functions of RSF1. It is therefore of interest to investigate whether the RSF1 21KR is exclusively deficient for SUMOylation. An alternative way for the disruption of SUMOylation sites that leaves the PTM-acceptor lysines intact,

is to mutate glutamate (E) to alanine (A) within the SUMO consensus sites [ExK;KxE]. Unfortunately only 17 sites out of the 21 mutated lysines within the RSF1 21KR sequence belong to a consensus motif containing a glutamate (Tabel S1).
Another important point is that two mutated lysines, K468 and K565 fit the Phosphorylation-Dependent SUMOylation Motif (PDSM) [KxExx(pS)P] (Table S1), with S473 and S570, being the phosphorylation-acceptor serine (S) in these motifs, respectively (Table S2). Whether the loss of SUMOylation at these phosphorylation-dependent sites influences a particular function of RSF1, is currently unknown. Interestingly, also other PTMs can have a stimulatory or repressive effect on the SUMOylation of target proteins. Phosphorylation frequently acts in a stimulating way through PDSMs, even at the single serine residue level (Flotho and Melchior, 2013). However, the role of crosstalk between SUMOylation and other PTMs on the function of RSF1 has not been investigated so far.
Recruitment of the RSF1 21KR mutant to DSBs
The RSF1 21KR mutant was recruited to laser-induced DSBs with the same kinetics as wild-type RSF1, suggesting that the recruitment of RSF1 to DNA damage is not dependent on its SUMOylation. Previous studies have shown that the recruitment of RSF1 mainly depends on ATM-mediated phosphorylation on S524, S1226 and S1325 (Matsuoka et al., 2007; Min et al., 2014; Pessina and Lowndes, 2014). These results also implicate that ATM-dependent phosphorylation of RSF1 upon DSB induction is not disturbed by the K to R mutations within the RSF1 21KR mutant, although this is not experimentally tested. Conversely, SUMOylation could also simply occur after RSF1 recruitment, and recruitment would therefore not be affected.

The RSF1 21KR mutant might be unable to recruit XRCC4
We observed a clear decrease in XRCC4 accumulation to the targeted RSF1 21KR mutant compared to RSF1 wt in LacO array-containing U2OS 2-6-3 cells (Fig. 3). As this recruitment was in the absence of DSBs, we can only speculate on the role of RSF1 SUMOylation in the process of DSB repair via NHEJ and the recruitment of XRCC4 to damaged chromatin. Nonetheless, a clear co-localization of XRCC4 and RSF1 wt was detected (Helfricht et al., 2013), which was abrogated within the RSF1 21KR SUMO mutant expressing cells (Fig. 3). Since SUMOylation was suggested to have a glue-like character promoting protein-protein interactions within diverse pathways (Jentsch and Psakhye, 2013), we wondered whether XRCC4 might bind to SUMOylated RSF1 during NHEJ. Surprisingly, using the GPS-SUMO tool that predicts SUMOylation sites and SIMs based on a proteins sequence, no SIM was predicted for XRCC4. Also the sequences of the centromere proteins CENP-S and CENP-X, which are deposited at DSBs by RSF1 to promote XRCC4 recruitment (Helfricht et al., 2013), appear to lack SIM domains. Hence, the binding of DSB-repair proteins to SUMOylated RSF1 upon DSB induction does not seem likely.
Importantly, we cannot exclude the possibility that the 21 K to R point mutations might lead to differences in protein folding, which possibly could interrupt direct or indirect interactions of RSF1 with other proteins and might affect XRCC4 loading. Thus, observations made with this artificial targeting approach need to be confirmed using a different experimental approach, showing that RSF1 SUMOylation is indeed involved in XRCC4 recruitment upon DSB induction.

It is furthermore noteworthy that SUMOylation-deficient mutant proteins frequently lack severe phenotypes (Sacher et al., 2006; Silver et al., 2011). Accordingly, Psakhye et al. found that a wave of SUMOylation events is triggered upon DNA damage

induction (Psakhye and Jentsch, 2012). Instead of individual proteins, several repair proteins within the HR pathway had been SUMOylated, often at multiple sites. Together, this supports a model where strictly controlled SUMOylation acts in a glue-like manner on closely located substrates to stabilize protein complexes by facilitating physical interactions (Psakhye and Jentsch, 2012). Which phenotypes are associated with SUMOylation deficient RSF1 and whether RSF1 contributes to the stability of protein interactions during DSB repair however remain to be investigated.

Identification of a SUMO E3 ligase for RSF1

Another unaddressed point is the identity of a SUMO E3 ligase responsible for RSF1 SUMOylation upon DNA-damage induction. PIAS1 and PIAS4 are likely candidates to facilitate RSF1 SUMOylation, due to the fact that they have been implicated in the DSB response (Galanty et al., 2009). Unfortunately, no investigation towards the identification of the SUMO ligase of RSF1 has been initiated yet. But to monitor the SUMOylation levels of RSF1 and the subsequent recruitment of XRCC4 to DSBs in cells depleted from PIAS1 and/or PIAS4, would provide useful information on the requirement of one or both of these SUMO ligases for RSF1 SUMOylation.

Potential strategies for future functional studies

Efforts to generate experimental data to elucidate a possible function of RSF1 SUMOlyation in the DDR were inconclusive. Expression of a siRNA-resistant version of RSF1 wt did not complement the knockdown-induced reduction of XRCC4 recruitment to DSB-containing laser tracks (Fig. S2). This could have had several reasons, one being inappropriate expression levels of RSF1. Not only does the depletion of RSF1 leads to defects in the response to DNA damage, the overexpression of RSF1 actually induces DNA damage (i.e. γH2AX), thereby initiating cell growth arrest and apoptosis (Sheu et al., 2010). For such complementation approaches, near-endogenous expression levels of RSF1 wt and 21KR mutant are therefore vital and further investigations are required to proof the functionality of tagged RSF1 and the importance of RSF1 SUMOylation when compared to RSF1 21KR mutant during complementation experiments.

An alternative approach to search for DNA damage-dependent interactors of RSF1 wt and 21KR would be either employing Co-IPs or mass spectrometry (MS) analysis. Possible SUMOylation-dependent interactors could be identified in this manner and the question, whether RSF1 recruits XRCC4 directly or indirectly via a NHEJ protein, could be addressed.

Besides promoting NHEJ upon DSB induction, RSF1 has also been suggested to be required for efficient HR (Helfricht et al., 2013; Min et al., 2014). This study so far however only focused on the possible involvement of RSF1 SUMOylation during NHEJ, which was based on former results (Helfricht et al., 2013). But RSF1 has also been suggested to promote the recruitment of the HR factors RPA and RAD51 to laser-induced DSBs (Min et al., 2014). Whether SUMOylation of RSF1 plays a role in the HR pathway however requires further investigation. Thus additional efforts have to be made in order to dissect the role of RSF1 SUMOylation during the DSB response via NHEJ as well as HR. Additionally, it would be interesting to research whether SUMOylation of RSF1 is specific for DSBs or occurs more globally in response to various types of DNA damage.

MATERIAL AND METHODS

Cell culture
U2OS cells and U2OS 2-6-3 cells containing a 200x integrated Lac operator genomic array were grown in DMEM (Gibco) containing 10% FCS (Bodinco BV) and 1% penicillin/streptomycin unless stated otherwise. U2OS 2-6-3 cells were a gift from Susan Janicki (Shanbhag et al., 2010) and were grown in DMEM supplemented with G418 [400 μg/ml].

Plasmids
The cDNA for human RSF1 in the vector pENTR223.1 was obtained from Open Biosystems and cloned into pDEST-EGFP-C1-STOP, a generous gift from Jason Swedlow, using the GATEWAY® system as described before (Helfricht et al., 2013). The mCherry-LacR encoding sequence from the mCherry-LacR-C1 vector (Coppotelli et al., 2013) and pDEST-EGFP-RSF1wt were digested by AgeI/XhoI and fused to generate the pDEST-mCherry-LacR-RSF1wt vector. Both constructs were made siRNA resistant to siRSF1-3 using site-directed mutagenesis to introduce 8 silent mutations.
The siRSF1-3-resistant RSF1 21KR sequence, flanked by suitable restriction sites, was synthesized by Genscript. This 21KR encoding sequence was swapped with the wt sequence by XhoI and PmlI digestion, purification and re-ligation into pDEST-GFP-RSF1. The RSF1 21KR insert of construct pDEST-EGFP-RSF1 21KR was cloned into the vector pDEST-mCherry-LacR using the restriction enzymes AgeI/XhoI generating the plasmid pDEST-mCherry-LacR-RSF1 21KR.
The NLS-sequence was cloned into GFP in a pEGFP-C1 vector and GFP-XRCC4 was kindly provided by Penny Jeggo (Girard et al., 2004).

Transfections and RNAi interference
siRNA and plasmid transfections were performed using Lipofectamine RNAiMAX (Invitrogen) or Lipofectamine 2000 (Invitrogen), respectively, according to the manufacturer's instructions. During the follow-up study, the following siRNA sequences were used:

5'- CGUACGCGGAAUACUUCGA -3' (Luciferase, Dharmacon),
5'- AGACAAAGGAAGAGAGCTA -3' (RSF1-3, Dharmacon).

Cells were transfected twice with siRNAs [40 nM] within 24 h and examined further 48 h after the second transfection, unless stated otherwise.

Immunoprecipitation
Flag-IPs were performed as previously described (Schimmel et al., 2014), lysing U2OS cells in four pellet volumes of lysis buffer (1% SDS, 0.5% NP-40 in PBS, including phosphatase and protease inhibitors). 70 mM Chloroacetamide was added freshly to Flag-IP lysates. After sonication, samples were incubated for 30 minutes at room temperature, followed by sample equalization using BCA Protein Assay Reagent (Thermo Scientific). 30 μl of each lysate was taken and stored as input sample. An equal volume of dilution buffer (2% Triton X-100, 0.5% sodium deoxycholate, 1% BSA, freshly added 70 mM chloroacetamide, 5 mM sodium fluoride, 1 mM sodium orthovanadate, 5 mM β-glycerol phosphate, 5 mM sodium pyrophosphate, 0.5 mM EGTA, 5 mM 1,10-phenanthroline, protease inhibitor including EDTA (Roche; 1 tablet per 10 ml buffer) was added to the lysates. Subsequently, samples

were centrifuged for 45 minutes at 13.2 krpm at 4°C. The supernatant was transferred to a clean tube and mixed with prewashed Flag-M2 beads (Sigma; 30 µl beads per 1 ml of diluted sample). Tubes were left rolling during incubation at 4°C for 90 minutes. Next, the beads were washed 5x with wash buffer (50 mM Tris, 150 mM NaCl, 70 mM chloroacetamide, 0.5% NP-40, 5 mM sodium fluoride, 1 mM sodium orthovanadate, 5 mM β-glycerolphosphate, 5 mM sodium pyrophosphate, 0.5 mM EGTA, 5 mM 1,10-phenanthrolineprotease inhibitor including EDTA (Roche; 1 tablet per 10 ml buffer)), including 3 tube changes. The Flag-SUMO-2 conjugates were eventually eluted with one bead volume of 5% SDS and 1 mM Flag M2 epitope peptide in wash buffer.

Purification of His-SUMO conjugates

U2OS cells stably expressing His-SUMO-2 were rinsed with and collected in icecold PBS. To prepare input samples, small aliquots of cells were lysed in 1x LDS sample buffer. For cell lysis, Guanidinium lysis buffer (6 M guanidinium-HCl, 0.1 M Na2HPO4/NaH2PO4, 0.01 M Tris/HCl, pH 8.0 and competing imidazole) was added to the cell pellet, followed by sonication to reduce the viscosity. The protein concentration of these lysates was subsequently determined using the BCA kit to equalize the samples. The His-SUMO-2 conjugates were enriched on nickel-nitrilotriacetic acid-agarose beads (Qiagen), which were subjected to washing using buffers A to D. Wash buffer A: 6 M guanidinium-HCl, 0.1 M Na2HPO4/NaH2PO4, 0.01 M Tris/HCl, pH 8.0, 10 mM β-mercaptoethanol, 0.3% Triton X-100. Wash buffer B: 8 M urea, 0.1 M Na2HPO4/NaH2PO4, 0.01 M Tris/HCl, pH 8.0, 10 mM β-mercaptoethanol, 0.3% Triton X-100. Wash buffer C: 8 M urea, 0.1 M Na2HPO4/NaH2PO4, 0.01 M Tris/HCl, pH 6.3, 10 mM β-mercaptoethanol, 0.3% Triton X-100. Wash buffer D: 8 M urea, 0.1 M Na2HPO4/NaH2PO4, 0.01 M Tris/HCl, pH 6.3, 10 mM β-mercaptoethanol, 0.1% Triton X-100. Eventually, samples were eluted in 7 M urea, 0.1 M Na2HPO4/NaH2PO4, 0.01 M Tris/HCl, pH 7.0, 500 mM imidazole.

GFP-IP

U2OS cells transiently expressing GFP, GFP-RSF1 wt or the 21KR mutant were either mock treated or exposed to 4 Gy of IR and incubated at 37°C for 1 h. Cells were trypsinized and washed in ice-cold PBS, followed by lysis in EBC buffer (50 mM Tris (pH 7.5), 150 mM NaCl, 0.5% NP-40, 1 mM EDTA, 5 mM 1,10-phenanthroline protease inhibitor including EDTA (Roche; 1 tablet per 10 ml buffer)) with 500 Units/ml Benzonase. Cell lysates were centrifuged for 10 min at full speed and cleared lysates were transferred to new tubes. For input sample preparation, 50 µl samples were transferred to new tubes and boiled in 2x Laemmli buffer at 95°C. Equal ammounts of GFP Trap beads (Chromotek) were added to cleared lysates for immunoprecipitation and incubated on a rotator for 1,5 h. Beads were subjected to 5 washing steps with EBC buffer [300mM NaCl] and eventually boiled in 2x Laemmli buffer at 95°C.

Antibodies

Western blot analysis was performed using antibodies against RSF1 (1:10, #m38B5, provided by Marinela Perpelescu and Kinya Yoda (Perpelescu et al., 2009)), SUMO-2/3 (1:1000, as previously described produced by A.C. Vertegaal in collaboration with Eurogentec (Vertegaal et al., 2004)), GFP (1:5000, #290, Abcam). Immunofluorescence analysis was performed using antibodies against γH2AX (1:1000-2000, #07-164, Millipore) and XRCC4 (1:500, provided by Mauro Modesti and Dik van Gent (Mari et al., 2006; Modesti et al., 1999)).

Laser micro-irradiation

For multiphoton or UV-A laser micro-irradiation, the media of U2OS cells grown on 18 mm glass coverslips was replaced with CO2-independent Leibovitz L15 medium complemented with 10% FCS and 1% penicillin/streptomycin. Next, cells were placed in a Chamlide TC-A live-cell imaging chamber and were kept at 37°C during imaging. The multiphoton laser was implemented on a Leica SP5 confocal microscope to which an environmental chamber set to 37°C was fitted as had been described before (Helfricht et al., 2013). Briefly, DSB-containing tracks (1.5 μm width) were generated with a Mira modelocked Ti:Sapphire laser (λ = 800 nm, pulselength = 200 fs, repetition rate = 76 MHz, output power = 80 mW). Using LAS-AF software, cells were micro-irradiated with 1 iteration per pixel and images were recorded before and after laser irradiation until 180 sec. UV-A laser micro-irradiation was performed after sensitization of cells with 10 μM 5'-bromo-2-deoxyuridine (BrdU) for 24 h, as described (ref). A Leica DM IRBE widefield microscope stand (Leica) with an integrated pulsed nitrogen laser (Micropoint Ablation Laser System; Photonic Instruments, Inc) was used for DNA-damage induction. The pulsed nitrogen laser (16 Hz, 364 nm) was thereby directly coupled to the epifluorescence path of the microscope and focused through a Leica 40× HCX PLAN APO 1.25–0.75 oil-immersion objective. To strictly induce localized sub-nuclear DNA damage, the laser output power was set to 78 and 2 iterations per pixel were applied with the Andor software. Cells were incubated for 10 minutes at 37 °C and subsequently fixed with 4% formaldehyde before immunostaining.

Immunofluorescent labeling

Immunostaining of cells for γH2AX and XRCC4 was performed as described previously (Helfricht et al., 2013). Briefly, cells were grown on glass coverslips and treated as indicated in the figure legends. Consequently, cells were washed with PBS, fixed with 4% formaldehyde for 10 min and treated with 0.1% Triton X-100 in PBS for 5 min. Cells were rinsed with PBS and equilibrated in PBS containing BSA [5 g/l] and glycine [1.5 g/l) prior to immunostaining. Detection was made possible through the use of goat anti-mouse or goat anti-rabbit IgG coupled to Alexa 555 or 647 (Invitrogen Molecular probes). Samples were incubated with DAPI [0.1 μg/ml] and mounted using Polymount (Polysciences, Inc.).

Microscopy analysis

A Zeiss AxioImager M2 widefield fluorescence microscope was used for image acquisition of fixed samples. The microscope was equipped with 40×, 63×, and 100× PLAN APO (1.4 NA) oil-immersion objectives (Zeiss) and an HXP 120 metal-halide lamp used for excitation, as well as ZEN software (2012). The fluorescent probes could be detected using the following filters: DAPI (excitation filter: 350/50 nm, dichroic mirror: 400 nm, emission filter: 460/50 nm), GFP/Alexa 488 (excitation filter: 470/40 nm, dichroic mirror: 495 nm, emission filter: 525/50 nm), mCherry (excitation filter: 560/40 nm, dichroic mirror: 585 nm, emission filter: 630/75 nm), Alexa 555 (excitation filter: 545/25 nm, dichroic mirror: 565 nm, emission filter: 605/70 nm), Alexa 647 (excitation filter: 640/30 nm, dichroic mirror: 660 nm, emission filter: 690/50 nm).

REFERENCES

1. Bekker-Jensen,S., Rendtlew,D.J., Fugger,K., Gromova,I., Nerstedt,A., Lukas,C., Bartek,J., Lukas,J., and Mailand,N. (2010). HERC2 coordinates ubiquitin-dependent assembly of DNA repair factors on damaged chromosomes. Nat. Cell Biol. 12, 80-86.
2. Choudhary,C., Kumar,C., Gnad,F., Nielsen,M.L., Rehman,M., Walther,T.C., Olsen,J.V., and Mann,M. (2009). Lysine acetylation targets protein complexes and co-regulates major cellular functions. Science 325, 834-840.
3. Coppotelli,G., Mughal,N., Callegari,S., Sompallae,R., Caja,L., Luijsterburg,M.S., Dantuma,N.P., Moustakas,A., and Masucci,M.G. (2013). The Epstein-Barr virus nuclear antigen-1 reprograms transcription by mimicry of high mobility group A proteins. Nucleic Acids Res. 41, 2950-2962.
4. Danielsen,J.R., Povlsen,L.K., Villumsen,B.H., Streicher,W., Nilsson,J., Wikstrom,M., Bekker-Jensen,S., and Mailand,N. (2012). DNA damage-inducible SUMOylation of HERC2 promotes RNF8 binding via a novel SUMO-binding Zinc finger. J. Cell Biol. 197, 179-187.
5. Flotho,A. and Melchior,F. (2013). Sumoylation: a regulatory protein modification in health and disease. Annu. Rev. Biochem. 82, 357-385.
6. Galanty,Y., Belotserkovskaya,R., Coates,J., Polo,S., Miller,K.M., and Jackson,S.P. (2009). Mammalian SUMO E3-ligases PIAS1 and PIAS4 promote responses to DNA double-strand breaks. Nature 462, 935-939.
7. Girard,P.M., Kysela,B., Harer,C.J., Doherty,A.J., and Jeggo,P.A. (2004). Analysis of DNA ligase IV mutations found in LIG4 syndrome patients: the impact of two linked polymorphisms. Hum. Mol. Genet. 13, 2369-2376.
8. Helfricht,A., Wiegant,W.W., Thijssen,P.E., Vertegaal,A.C., Luijsterburg,M.S., and van Attikum,.H. (2013). Remodeling and spacing factor 1 (RSF1) deposits centromere proteins at DNA double-strand breaks to promote non-homologous end-joining. Cell Cycle 12, 3070-3082.
9. Hendriks,I.A., D'Souza,R.C., Yang,B., Verlaan-de,V.M., Mann,M., and Vertegaal,A.C. (2014). Uncovering global SUMOylation signaling networks in a site-specific manner. Nat. Struct. Mol. Biol. 21, 927-936.
10. Hendriks,I.A., Treffers,L.W., Verlaan-de,V.M., Olsen,J.V., and Vertegaal,A.C. (2015). SUMO-2 Orchestrates Chromatin Modifiers in Response to DNA Damage. Cell Rep.
11. Hu,X., Paul,A., and Wang,B. (2012). Rap80 protein recruitment to DNA double-strand breaks requires binding to both small ubiquitin-like modifier (SUMO) and ubiquitin conjugates. J. Biol. Chem. 287, 25510-25519.
12. Jackson,S.P. and Durocher,D. (2013). Regulation of DNA damage responses by ubiquitin and SUMO. Mol. Cell 49, 795-807.
13. Jentsch,S. and Psakhye,I. (2013). Control of nuclear activities by substrate-selective and protein-group SUMOylation. Annu. Rev. Genet. 47, 167-186.
14. Lan,L., Ui,A., Nakajima,S., Hatakeyama,K., Hoshi,M., Watanabe,R., Janicki,S.M., Ogiwara,H., Kohno,T., Kanno,S., and Yasui,A. (2010). The ACF1 complex is required for DNA double-strand break repair in human cells. Mol. Cell 40, 976-987.
15. Luijsterburg,M.S., Acs,K., Ackermann,L., Wiegant,W.W., Bekker-Jensen,S., Larsen,D.H., Khanna,K.K., van Attikum,H., Mailand,N., and Dantuma,N.P. (2012). A new non-catalytic role for ubiquitin ligase RNF8 in unfolding higher-order chromatin structure. EMBO J. 31, 2511-2527.
16. Luo,K., Zhang,H., Wang,L., Yuan,J., and Lou,Z. (2012). Sumoylation of MDC1 is important for proper DNA damage response. EMBO J. 31, 3008-3019.
17. Mari,P.O., Florea,B.I., Persengiev,S.P., Verkaik,N.S., Bruggenwirth,H.T., Modesti,M., Giglia-Mari,G., Bezstarosti,K., Demmers,J.A., Luider,T.M., Houtsmuller,A.B., and van Gent,D.C. (2006). Dynamic assembly of end-joining complexes requires interaction between Ku70/80 and XRCC4. Proc. Natl. Acad. Sci. U. S. A 103, 18597-18602.
18. Matic,I., Schimmel,J., Hendriks,I.A., van Santen,M.A., van de Rijke,F., van,D.H., Gnad,F., Mann,M., and Vertegaal,A.C. (2010). Site-specific identification of SUMO-2 targets in cells reveals an inverted SUMOylation motif and a hydrophobic cluster SUMOylation motif. Mol. Cell 39, 641-652.
19. Matsuoka,S., Ballif,B.A., Smogorzewska,A., McDonald,E.R., Hurov,K.E., Luo,J., Bakalarski,C.E., Zhao,Z., Solimini,N., Lerenthal,Y., Shiloh,Y., Gygi,S.P., and Elledge,S.J. (2007). ATM and ATR substrate analysis reveals extensive protein networks responsive to DNA damage. Science 316, 1160-1166.
20. Min,S., Jo,S., Lee,H.S., Chae,S., Lee,J.S., Ji,J.H., and Cho,H. (2014). ATM-dependent chromatin remodeler Rsf-1 facilitates DNA damage checkpoints and homologous recombination repair. Cell Cycle 13, 666-677.
21. Modesti,M., Hesse,J.E., and Gellert,M. (1999). DNA binding of Xrcc4 protein is associated with V(D)J recombination but not with stimulation of DNA ligase IV activity. EMBO J. 18, 2008-2018.
22. Morris,J.R., Boutell,C., Keppler,M., Densham,R., Weekes,D., Alamshah,A., Butler,L., Galanty,Y., Pangon,L., Kiuchi,T., Ng,T., and Solomon,E. (2009). The SUMO modification pathway is involved in the BRCA1 response to genotoxic stress. Nature 462, 886-890.
23. Perpelescu,M., Nozaki,N., Obuse,C., Yang,H., and Yoda,K. (2009). Active establishment of centromeric CENP-A chromatin by RSF complex. J. Cell Biol. 185, 397-407.
24. Pessina,F. and Lowndes,N.F. (2014). The RSF1 histone-remodelling factor facilitates DNA double-strand break repair by

recruiting centromeric and Fanconi Anaemia proteins. PLoS. Biol. 12, e1001856.
25. Psakhye,I. and Jentsch,S. (2012). Protein group modification and synergy in the SUMO pathway as exemplified in DNA repair. Cell 151, 807-820.
26. Sacher,M., Pfander,B., Hoege,C., and Jentsch,S. (2006). Control of Rad52 recombination activity by double-strand break-induced SUMO modification. Nat. Cell Biol. 8, 1284-1290.
27. Saitoh,H. and Hinchey,J. (2000). Functional heterogeneity of small ubiquitin-related protein modifiers SUMO-1 versus SUMO-2/3. J. Biol. Chem. 275, 6252-6258.
28. Schimmel,J., Eifler,K., Sigurethsson,J.O., Cuijpers,S.A., Hendriks,I.A., Verlaan-de,V.M., Kelstrup,C.D., Francavilla,C., Medema,R.H., Olsen,J.V., and Vertegaal,A.C. (2014). Uncovering SUMOylation dynamics during cell-cycle progression reveals FoxM1 as a key mitotic SUMO target protein. Mol. Cell 53, 1053-1066.
29. Shanbhag,N.M., Rafalska-Metcalf,I.U., Balane-Bolivar,C., Janicki,S.M., and Greenberg,R.A. (2010). ATM-dependent chromatin changes silence transcription in cis to DNA double-strand breaks. Cell 141, 970-981.
30. Sheu,J.J., Guan,B., Choi,J.H., Lin,A., Lee,C.H., Hsiao,Y.T., Wang,T.L., Tsai,F.J., and Shih,I. (2010). Rsf-1, a chromatin remodeling protein, induces DNA damage and promotes genomic instability. J. Biol. Chem. 285, 38260-38269.
31. Silver,H.R., Nissley,J.A., Reed,S.H., Hou,Y.M., and Johnson,E.S. (2011). A role for SUMO in nucleotide excision repair. DNA Repair (Amst) 10, 1243-1251.
32. Smeenk,G., Wiegant,W.W., Marteijn,J.A., Luijsterburg,M.S., Sroczynski,N., Costelloe,T., Romeijn,R.J., Pastink,A., Mailand,N., Vermeulen,W., and van Attikum,.H. (2013). Poly(ADP-ribosyl)ation links the chromatin remodeler SMARCA5/SNF2H to RNF168-dependent DNA damage signaling. J. Cell Sci. 126, 889-903.
33. Song,J., Durrin,L.K., Wilkinson,T.A., Krontiris,T.G., and Chen,Y. (2004). Identification of a SUMO-binding motif that recognizes SUMO-modified proteins. Proc. Natl. Acad. Sci. U. S. A 101, 14373-14378.
34. Soutoglou,E. and Misteli,T. (2008). Activation of the cellular DNA damage response in the absence of DNA lesions. Science 320, 1507-1510.
35. Strauss,C. and Goldberg,M. (2011). Recruitment of proteins to DNA double-strand breaks: MDC1 directly recruits RAP80. Cell Cycle 10, 2850-2857.
36. Strauss,C., Halevy,T., Macarov,M., Argaman,L., and Goldberg,M. (2011). MDC1 is ubiquitylated on its tandem BRCT domain and directly binds RAP80 in a UBC13-dependent manner. DNA Repair (Amst) 10, 806-814.
37. Vertegaal,A.C., Ogg,S.C., Jaffray,E., Rodriguez,M.S., Hay,R.T., Andersen,J.S., Mann,M., and Lamond,A.I. (2004). A proteomic study of SUMO-2 target proteins. J. Biol. Chem. 279, 33791-33798.

SUPPLEMENTAL INFORMATION

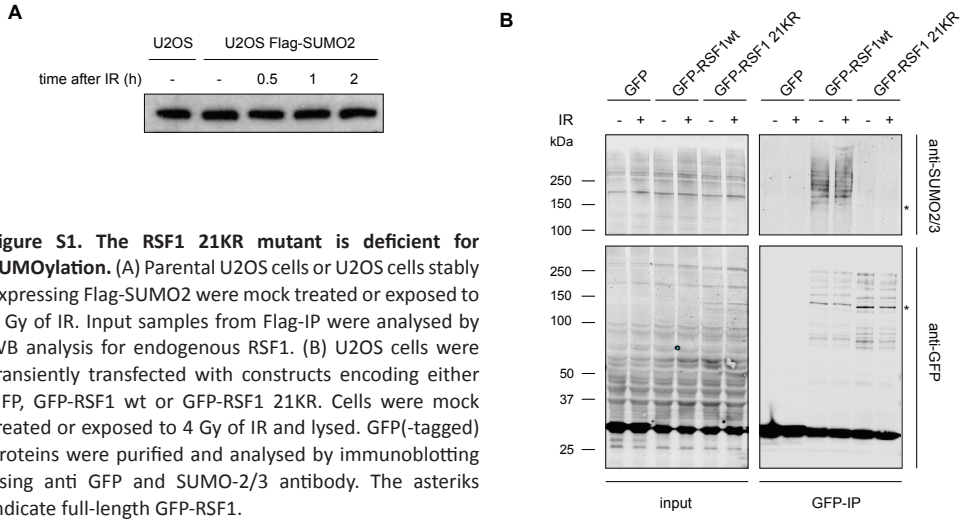

Figure S1. The RSF1 21KR mutant is deficient for SUMOylation. (A) Parental U2OS cells or U2OS cells stably expressing Flag-SUMO2 were mock treated or exposed to 4 Gy of IR. Input samples from Flag-IP were analysed by WB analysis for endogenous RSF1. (B) U2OS cells were transiently transfected with constructs encoding either GFP, GFP-RSF1 wt or GFP-RSF1 21KR. Cells were mock treated or exposed to 4 Gy of IR and lysed. GFP(-tagged) proteins were purified and analysed by immunoblotting using anti GFP and SUMO-2/3 antibody. The asteriks indicate full-length GFP-RSF1.

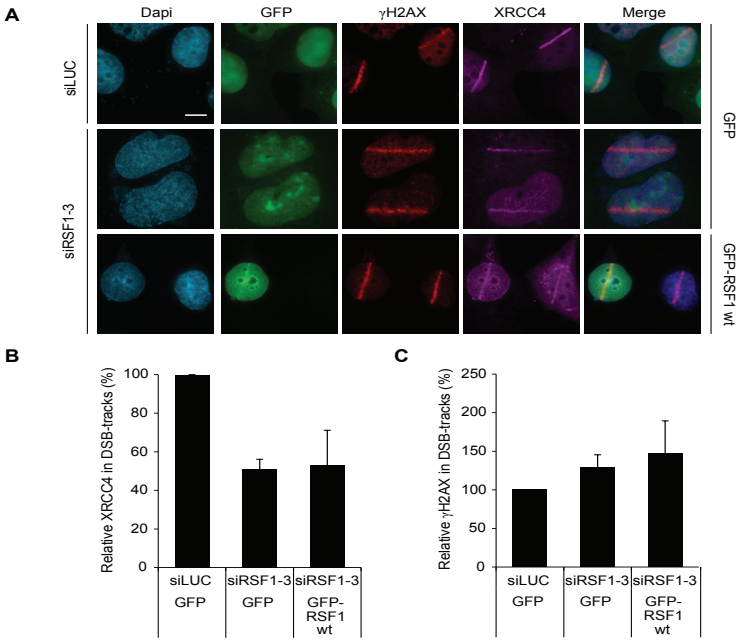

Figure S2. Exogenous RSF1 wt fails to complement the XRCC4 recruitment defect of U2OS cells depleted from endogenous RSF1. (A) U2OS cells were treated with siLuc or siRSF1-3 for 48 h and were subsequently transfected with constructs encoding GFP or GFP-RSF1 wt. After 24 h, cells were locally irradiated with an UV-A laser and fixed after 10 min followed by immunostaining for γH2AX, XRCC4 and Dapi. Mounted cells were analysed with a wide-field microscope and representative images are shown. The scale bar indicates 10 µm. (B) Quantification of the amount of XRCC4 recruitment to DSB-containing laser tracks of cells in (A). The average of three independent experiments is presented, in which more than 45 cells have been analysed. The error bars represent the s.e.m. (C) As in (B) only that γH2AX recruitment was measured.

Tabel S1. List of SUMO target sites mutated in RSF1 21KR. (A) Listed are identified SUMO target sites and additional inverted motifs, ([1]Hendriks et al., 2014). Blue: Lysine fitting the Phosphorylation-dependent SUMOylation motif (PDSM) [KxExx(pS)P], Red: SUMO acceptor lysine not belonging to glutamate (E)-containing SUMO consensus motifs. (B) Listed are SIMs in the amino acid (aa) sequence of RSF1 predicted by the GPS-SUMO tool.

Nr.	SUMO sites[1] Lysine position	aa sequence
1	K243	EETP**K**QEEQ
2	K254	SEKM**K**SEEQ
3	K277	ETTV**K**KEKE
4	K280	VKKE**K**EDEK
5	K294	PVIC**K**LEKP
6	K306	NEEK**K**IIKE
7	K309	KKII**K**EESD
8	K323	VKPI**K**VEVK
9	K337	PKDT**K**SSM
10	K358	GGNI**K**SSHE
11	K390	KREI**K**LSDD
12	K415	KEFL**K**DEIK
13	K419	KDEI**K**QEEE
14	K456	APNF**K**TEPI
15	K463	PIET**K**FYET
16	K468	FYET**K**EESY
17	K565	SCTM**K**GEEK
18	K670	LETL**K**EDSE
19	K677	SEFT**K**VEMD
20	K758	EPEN**K**QEKT
21	K768	KEEE**K**TNVG

PDSM ≠ ExK or KxE

Tabel S2. List of described phosphorylation and acetylation target sites found in RSF1.
www.phosphosite.org.
Yellow: ATM-/ATR phosphorylation target sites ([1]Matsuoka et al., 2007, [2]Choudhary et al., 2009).

Nr.	Phosphorylation sites[1] erine/Threonine positior	Acetylation sites[2] Lysine prosition
1	S392	K1050
2	S397	K1339
3	T408	
4	S473	
5	S524	
6	S570	
7	S604	
8	S622	
9	S629	
10	S748	
11	S1221	
12	S1223	
13	S1226	
14	S1245	
15	S1277	
16	T1278	
17	Y1281	
18	S1282	
19	T1305	
20	S1310	
21	S1325	
22	S1345	
23	S1359	
24	S1375	

ATM-/ATR-target sites